Multi-lipid synergy in biolubrication: natural redundancy vs. natural selection

Multi-lipid synergy in biolubrication: natural redundancy vs. natural selection

Yifeng Cao[1,2,†], Di Jin[1,†], Nir Kampf[1], and Jacob Klein[1]*

1. Department of Molecular Chemistry and Materials Science, Weizmann Institute of Science, Rehovot 76100, Israel
2. Present address: Institute of Zhejiang University-Quzhou, Quzhou 324000, China; College of Chemical and Biological Engineering, Zhejiang University, Hangzhou 310027, China.

*To whom correspondence should be addressed: jacob.klein@weizmann.ac.il.

† Equal contribution

Abstract:

Phospholipid surface assemblies are crucial ingredients in reducing the boundary friction of articular cartilage in synovial joints such as hips and knees, of central importance to their homeostasis and to tissue-wear-related diseases such as osteoarthritis. From the point of view of biolubrication, the very large number of different lipids in joints begs the question of whether this is natural redundancy, or does this multiplicity confer any benefits, possibly through natural selection. Here we demonstrate that particular combinations of lipids present in joints may carry a clear benefit for their lubricating properties. Using progressively more complex mixtures of lipids representative of those in joints, and measuring their interactions using a uniquely-sensitive surface forces balance at physiologically-relevant salt concentrations and pressures, we show that different lipid combinations lead to very significant differences in their efficacy as boundary lubricants. This points to a clear synergy arising from the multiple lipid types in the lubricating layers, provides insight into the role of lipid type proliferation in synovial joints, of possibly evolutionary origins, and may suggest new treatment modalities for osteoarthritis. We identify parameters of lipid-based boundary layers that might contribute to improved boundary lubrication in the light of the present study. Finally, we describe a possible approach based on molecular dynamics (MD) to emulating such optimal lipid combinations, and provide proof-of-concept MD simulations to illustrate this approach.

Keywords: Biolubrication; phospholipid mixtures; surface forces; hydration lubrication; hemifusion; lubrication synergy; synovial joints; osteoarthritis.

Introduction

Synovial joints, such as hips and knees, have evolved as long-lived, highly efficient lubrication systems under physiological conditions, and the resulting low friction at the articular cartilage surface, with sliding friction coefficients μ (= [force to slide]/[load]) as low, or even lower than 0.001, is crucial for their homeostasis[1, 2]. In particular it is of central importance for suppressing wear-related cartilage degradation, a leading symptom of osteoarthritis, the most widespread joint pathology[2]. The highly lubricious nature of the articular cartilage layers coating the ends of the joint bones, which slide past each other as the joints articulate, is due both to the role of interstitial fluid pressure within the cartilage, and largely to strongly-lubricating boundary layers at the cartilage surface, whose molecular origins have been extensively studied[2, 3, 4, 5, 6]. In recent years, surface-attached phospholipid layers, in particular phosphatidylcholines (PCs), which are ubiquitous in joints, have been shown to act as exceptionally good boundary lubricants at both synthetic and at biological surfaces[1, 7, 8, 9, 10]. Model studies have shown that both zwitterionic PCs[7, 10] and sphingomyelin (SM) lipids[11] in the form of single-component, surface-adsorbed vesicles or bilayers, exposing their highly hydrated headgroups at the slip-plane, can impart lubrication capability up to physiological pressures, with μ down to 10^{-4} or lower, which is equivalent to that of articular cartilage in synovial joints. The friction-reduction properties of such layers arise through the hydration lubrication mechanism[12] active at the highly-hydrated phosphocholine groups exposed by surface-attached boundary layers incorporating these lipids[13, 14]. It has been proposed that similar boundary layers are present at the articular cartilage surface, providing its excellent lubricity[1, 2, 15]. Studies of boundary lubrication by phospholipids have all, with few exceptions[16, 17, 18], examined single-component PCs[4, 7, 10, 13, 19, 20]. Healthy joints, however, are known to include lipids belonging to many different classes, comprising additionally different tail saturation levels and lengths[21, 22, 23,

[24]. While lipids have many biological functions, our main interest here is their contribution to joint lubrication. A key question, therefore, which this study seeks to address, is whether - separately from any other biological functions - this proliferation of different lipids in joints holds benefits for boundary lubrication at the articular cartilage surface, relative to the single or two-component PC layers which have been studied to date. A corollary to this question, which we also address, is whether, based on the results of this study, we may attempt to predict combinations of synovial lipids that can optimize their boundary lubrication performance.

The major phospholipid (PL) groups identified in synovial joints, present in the form of multilamellar and vesicular structures[25, 26] include electroneutral PC, SM, and phosphatidylethanolamine (PE), as well as minor components negatively charged PLs[21, 23], and the majority have at least one unsaturated tail[23], while the species and concentration of PLs in synovial joints are also affected by joint diseases, such as osteoarthritis (OA) and rheumatoid arthritis (RA)[27, 28]. The molecular structure of PLs modulates their properties, and considerable progress has been achieved in studying the relationship between the structure and lubrication efficiency of PCs[13, 29]. The phase state of a PC bilayer, i.e. whether in gel (more solid-like) or liquid (more fluid) state, is an important factor in the lubrication behavior of single-component PCs, with differing and sometimes opposing effects. Thus, on the one hand, fluid lipid bilayers are mechanically weaker and less robust to shear under physiologically high pressures, so are seemingly less suited as boundary lubricants[29]; while on the other hand their fluidity aids their healing following any damage or wear[10], which is clearly beneficial for sustained lubrication. Additionally, though they are mostly excellent boundary lubricants, single-component PC lipids in the gel- or in the fluid-phases behave differently depending on the nature of the substrates, whether hard (such as mica,

quartz, implant surfaces) or softer, e.g. biomimetic surfaces[13, 29, 30]. Moreover, a PL mixture with immiscible components may lead to phase-separated PL membranes[31], and thus frictional behavior different to that of a single-component PL. In a previous study, we examined the interactions between membranes of a binary mixture of 2 PC lipids: 1,2-dipalmitoyl-*sn*-glycero-3-phosphocholine (DPPC) and 1-palmitoyl-2-oleoyl-glycero-3-phosphocholine (POPC)[18]. In that system the phase separation facilitated hemifusion of the opposing layers, and the consequent elimination of the hydration-lubricated slip-plane at the headgroup-headgroup interface caused an abrupt increase in the friction force. Different salt ions also play an important role in joint lubrication. At the physiologically-high total salt concentration in the joints (ca. 150 mM), electrostatic interactions at the lipid headgroups are strongly screened; in addition, monovalent sodium cations may specifically adsorb to the surface of zwitterionic lipid bilayers[32]. Interaction of multivalent ions with PLs is more complex than that of monovalent cations, and is much stronger for negatively-charged (anionic) PLs than for zwitterionic ones[33]. In particular, while divalent cations ubiquitous in joints, such as calcium and magnesium, may modulate the charge property of PL membranes, and also act to bridge negatively-charged groups[34, 35].

The present study focuses on the forces acting between surface boundary layers of lipid mixtures, including the major PL classes found in healthy synovial fluid and on cartilage surfaces, to provide insight into the lubrication efficiency and possible synergy of multi-component lipid boundary layers. By synergy here is meant that the effect of combining different lipids leads to better lubrication than just the sum of the parts. In particular, while it is clearly not possible to test all possible combinations of the order of 100 or more different PLs in joints[21, 23, 24], a demonstration of improved lubrication arising from particular combinations of different lipids in the boundary layers

would provide insight from a biolubrication perspective as to the proliferation of different lipids in joints. Extending our previous work on single-component PLs and binary PC mixtures, we aim to mimic the diverse mixture of PLs in joints by adsorbing increasingly complex lipid mixtures (Fig. S1 and Table S1) on a model substrate, and measuring normal and frictional forces between them at physiological salt concentrations. Forces are measured using the surface force balance (SFB), where the model substrate is negatively charged, atomically-smooth mica.

Results

The three PL mixtures composed of 2, 5, and 8 PLs/lipids, designated L2, L5, and L8 respectively, were selected to include progressively more of the major lipid classes in synovial joints (Fig. S1 and Table S1). To approximately mimic the PLs in synovial joints, all the representative mixtures contain lipids with phosphocholine and phosphoethanolamine headgroups, which are the main lipid groups detected in the joints, as summarized in Fig. 1, and all have unsaturated PLs as majority

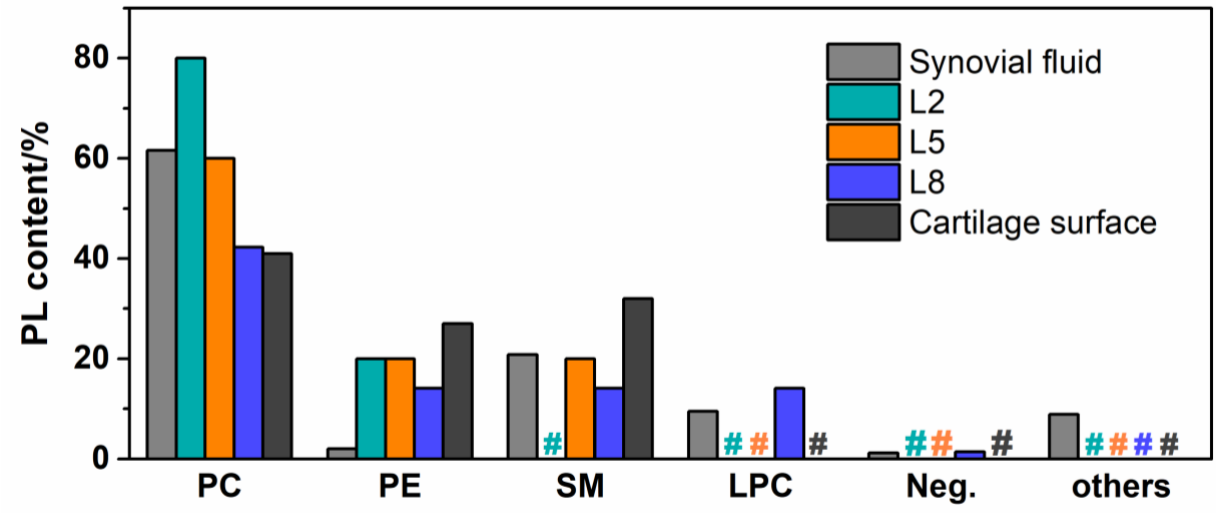

Figure 1. Major classes of PLs identified in synovial fluid (SF, light gray), on the cartilage surface (dark grey), as well as the L2, L5, and L8 systems in this study (green, orange, and purple, respectively). Neg. represents negatively charged PLs. Data were adapted from Refs. [21] and [23] for those on the cartilage surface and in synovial fluid, respectively. The black # symbols indicate the absence of the corresponding PLs on the cartilage surface, while coloured # indicate their absence from the lipid mixtures in this study.

components. L8 included, in addition to main PL types, also cholesterol which is ubiquitous in physiological lipid bilayers. To obtain deeper insight into the nature of the effect of combining the different lipids, as will be later considered, all measurements were carried out both in the absence and in the presence of calcium ions (as the $Ca(NO_3)_2$ salt) at their physiological concentrations. Size distribution and zeta potentials of SUVs of the three mixtures were characterized by DLS and are shown in Table 1, with all three having rather small negative potentials. We point out that addition of 2 mM $Ca(NO_3)_2$ had little effect on the DLS-measured vesicle diameters (which remained at ca. 65 nm) for L2 and L5, indicating little aggregation by the divalent ions. In contrast, L8, which included the negatively-charged DPPA (at low concentration – ca. 1.4 mole %) and had a slightly more negative zeta potential, was clearly aggregated by the calcium ions, which presumably acted as adhesive linkers between the DPPA headgroups on the vesicles. Formation of surface assemblies of the lipids on the mica substrate was achieved by spontaneous adsorption of the vesicles from the respective dispersions (Experimental Section), following which they ruptured to form bilayers on the mica[41]. Morphologies of these bilayers were characterized by AFM (Fig. 2). Normal and shear forces between the bilayer-bearing mica surfaces at different surface separations *D* across the respective SUV dispersions with and without added $Ca(NO_3)_2$ were directly measured using an SFB

(Figs. 3-4). Below we consider results for each mixture separately, then compare and summarize our conclusions at the end.

Table 1. Averaged size, PdI, and zeta potential values of mixed PLs/lipids-SUVs prepared in 150 mM $NaNO_3$ before and after adding $Ca(NO_3)_2$.

Lipid composition	**Dispersant**	**Size/nm**	**PdI**	**Zeta potential/mV**
POPC-POPE	150 mM $NaNO_3$	68.2 ± 1.2	0.064	-4.8 ± 1.6
	+ 2 mM $Ca(NO_3)_2$	69.6 ± 2.0	0.082	-2.3 ± 1.7
DPPC-POPC-DOPC-POPE-Egg SM	150 mM $NaNO_3$	65.1 ± 0.7	0.072	-1.6 ± 0.6
	+ 2 mM $Ca(NO_3)_2$	64.1 ± 1.1	0.066	-0.4 ± 0.2
DPPC-POPC-DOPC-POPE-Egg SM-DPPA-LPC-Chol	150 mM $NaNO_3$	63.4 ± 0.7	0.057	-7.3 ± 0.3
	+ 2 mM $Ca(NO_3)_2$	Multiple peaks	0.440	-5.3 ± 0.3

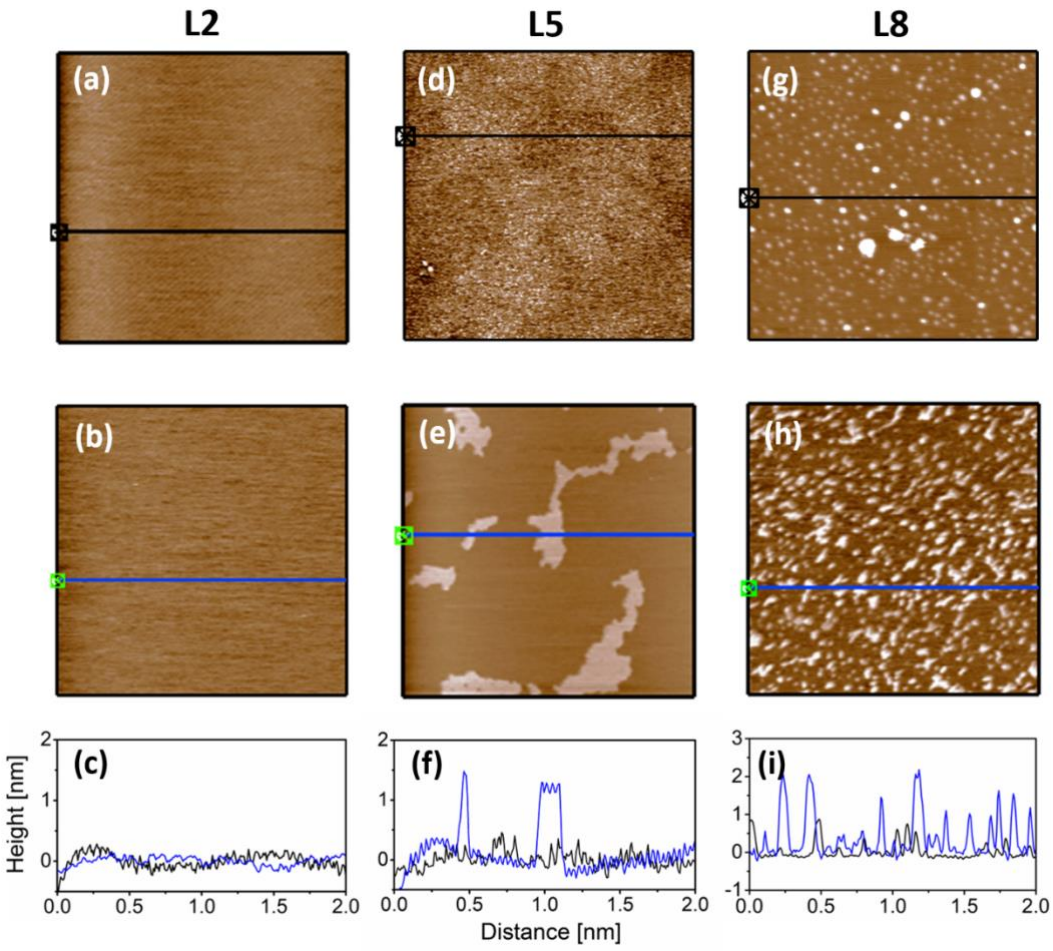

Figure 2. AFM height images of SUVs adsorbed on mica before (a, d, and g) and after (b, e, and h) adding 2 mM $Ca(NO_3)_2$ for the L2 (a-c), L5 (d-f), and L8 (g-i) systems, respectively. All scans were performed across 0.3 mM SUV dispersion prepared in 150 mM $NaNO_3$. The size of each image is 2 µm × 2 µm. Figures (c), (f), and (i) in the last row are corresponding height profiles, whereas the black and blue lines represent those before and after adding 2 mM $Ca(NO_3)_2$.

L2 mixture: POPC-POPE (4:1, molar ratio)

Phosphocholine and phosphoethanolamine are the two major lipid headgroup classes in synovial joints[21, 23], as seen in Fig. 1, and hydrophobic tails with one unsaturated group are the most common tail class. POPC and POPE in a molar ratio of 4:1 – roughly the ratio of phosphocholine and phosphoethanolamine headgroups in joints– were therefore selected as the first model mixture.

Compared with the well-studied POPC[42], POPE has a smaller headgroup and stronger inter-lipid hydrogen-bonding interactions, consequently leading to a more densely packed bilayer and thus lower area per headgroup, together with a higher phase transition temperature (Table S1)[43, 44]. Additionally, vesicles containing PEs have also been found to be more negative than electroneutral PC-vesicles[45], possibly due to the more inward headgroup orientation of PE compared with PC, exposing more of the negatively charged phosphate group at the surface[43, 44].

When mica is immersed in the POPC-POPE-SUV dispersion, planar bilayers of the POPC-POPE mixtures are formed on its surface (Figs. 2a and 2b). This is presumably because, despite the (small) net negative ζ-potential of the vesicles arising from the minority PE component[45], there is an attractive dipole-charge interaction with the negatively-charged mica attributed to the zwitterionic lipid headgroups of the majority PC component, leading to liposome adsorption and vesicle rupture. At 2 mM calcium concentration, both the non-aggregation of the vesicles and negative zeta potential values of the SUVs (Table 1, Fig. S2), as well as the unchanged morphology of supported bilayer on mica, indicate that Ca^{++} interacts only weakly with the POPC-POPE mixture. This is also consistent with a previous report[46].

Normal and shear force profiles were determined for all three mixtures between mica surfaces immersed in the respective vesicle dispersions, both with and without added calcium salt. Fig. 3 shows typical shear trace profiles for all three mixtures, while Figs. 4a and 4b shows the normal and friction force profiles for the L2 mixture.

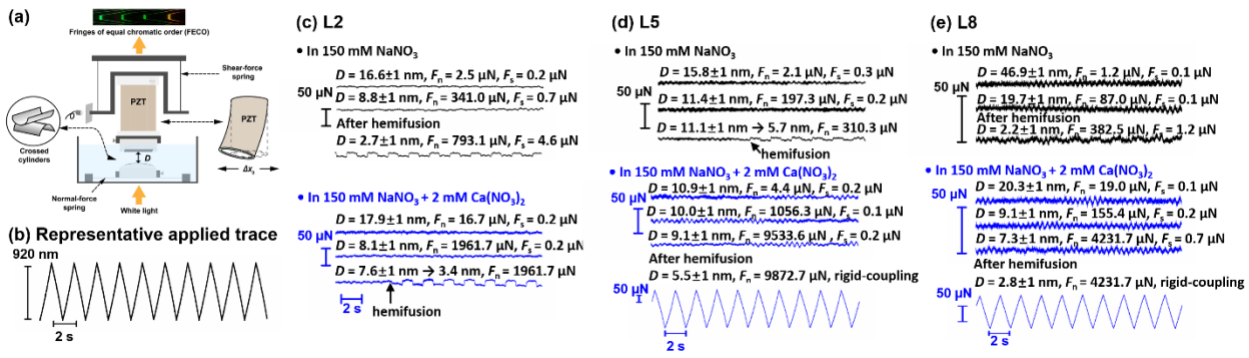

Figure 3. Illustration of the SFB setup (a) and representative applied lateral motion to the upper surface (b), and shear force $F_s(t)$ traces (c-e) across L2, L5 and L8 dispersions, respectively. In panel (a), two mica surfaces are in a crossed-cylindrical configuration at a closest separation distance D, which is determined according to the wavelengths of fringes of equal chromatic order (FECO) using the multiple beam interference technique (the fringes shown in the top panel are for two surfaces in adhesive contact). Normal and shear forces were determined by the bending of corresponding springs. Displacement of shear springs is monitored by an air-gap capacitor, as responses to the applied back-and-forth motion via the sectored PZT. In figures (c-e), black and blue traces represent those before and after adding 2 mM $Ca(NO_3)_2$. The changes in shear traces at hemifusion, indicated by an increase in F_s, were recorded for the L2 system after adding calcium (the lowest blue trace in (c), and for the L5 system before adding calcium (the lowest black trace in (d)). Hemifusion was observed after applying sufficient normal force to the system, and occasionally took place while recording the shear trace, as indicated by the arrows.

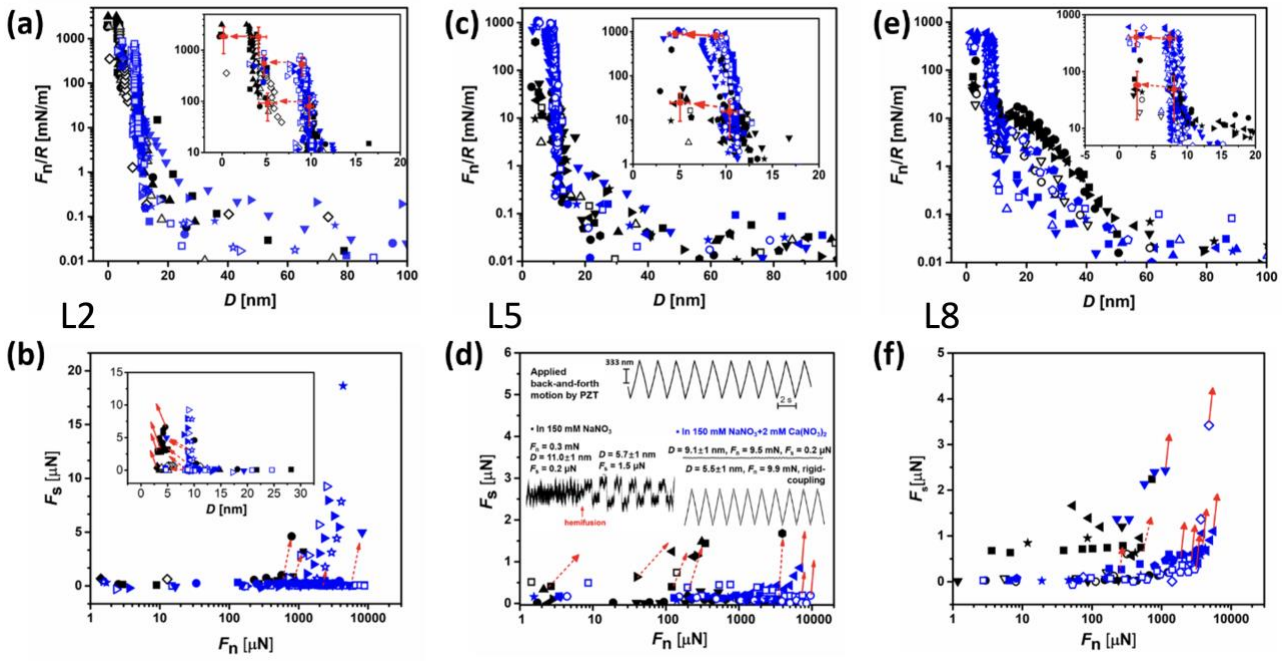

Figure 4. Force profiles across 0.3 mM L2 (a and b), L5 (c and d), and L8 (e and f) dispersion in 150 mM $NaNO_3$ before (black symbols) and after (blue symbols) adding 2 mM $Ca(NO_3)_2$, respectively. **(a, c, and e)** Normalized force versus separation distance (F_n/R vs. D) profiles. **(b, d, and f)** Shear force versus normal force (F_s vs. F_n) profiles, D = 0 nm is defined as mica-mica contact in air. Solid and open symbols represent the first and subsequent approaches, respectively. Arrows in the inset of figure (a, c, and e) indicate jumps in D when a bilayer is removed from the contact area by hemifusion (ca. 10 to 5 nm, broken lines) or totally squeezed out (ca. 5 to 0 nm, solid line). Data for figures (b, d, and f) were extracted from shear force traces as in Fig. 4, whereas red broken arrows indicate increases in F_s observed at hemifusion in 150 mM $NaNO_3$, while the red solid arrows indicate "rigid-coupling" of two surfaces at hemifusion following Ca^{++} addition, where F_s is higher than the detection limit of the device (185 μN) and "rigid-coupling" occurs (see text).

In Fig. 4a, the double-layer repulsion between the surfaces is strongly screened (Debye screening length ≈ 0.8 nm at 150 mM monovalent salt), and the normal forces acting between the POPC-POPE membranes are negligible at $D \gtrsim 13$ nm, a little greater than the thickness of two hydrated PL bilayers. This is consistent with the flat lipid bilayer structure observed by AFM scanning (Fig. 2a). As $F_n(D)$ increases, D decreases gradually until at a critical normal load, it shifts abruptly from 9.8

± 0.5 to 5.1 ± 1.0 nm, indicating that two PL bilayers hemifuse into one (inset to Fig. 4a). On further loading, the trapped bilayer is squeezed out of the contact area, as D decreases from 4.1 ± 0.9 nm to 0.2 ± 0.4 nm, revealing that the POPC-POPE bilayer adheres only weakly to the mica surface. On adding 2 mM calcium, the most striking change is that the normalized load ($F_n(D)/R$) that induces hemifusion increases more than 6-fold, from 80.4 ± 46.2 to 529.5 ± 207.0 mN/m, corresponding to pressures of a few MPa, comparable with those in synovial joints. Once hemifusion or total expulsion of the bilayer from the contact region occurred, force profiles following separation of the surfaces and successive approaches (empty symbols in Figs. 4a and 4b) are similar to those of the first approach, indicating that the POPC-POPE layer on each surface underwent self-healing to form a continuous bilayer again.

The shear force versus normal force profiles (F_s vs. F_n) between POPC-POPE bilayers are presented in Fig. 4b, and the shear force versus separation distance (F_s vs. D) profiles are inset to Fig. 4b. Before adding calcium, the shear forces are very low (at noise level) prior to hemifusion, while a significant increase is observed when hemifusion takes place. Following total expulsion of the lipid, the shear force increases abruptly and the two surfaces become rigidly coupled over the range of lateral motion applied to the top surface (so that sliding friction cannot be measured). Adding calcium can induce slightly higher shear forces prior to hemifusion, with friction coefficients in the range $0.004 \leq \mu \leq 0.0001$, possibly due to weak bridging of the exposed phosphocholine groups by the Ca^{++} ions, while hemifusion induces a clear increase in the friction forces, indicated by arrows with dashed lines in Fig. 4b. Compared with a previously reported POPC-DPPC mixture (4:1, molar ratio) where "rigid-coupling" was observed upon hemifusion[18], it is seen that DPPC adheres more strongly than POPE to the negatively charged substrate. The most

significant result here is the large increase in resistance to hemifusion (and its associated friction-increase) afforded by the presence of calcium ions, to which we return later.

L5 mixture: DPPC-POPC-DOPC-POPE-Egg SM (1:1:1:1:1, molar ratio)

The second system is composed of five zwitterionic PLs with different headgroup structures and unsaturation of the tails; DPPC, Egg SM, and POPE are in their gel-state, while POPC and DOPC are in the fluid (liquid crystalline)-state (Table S1). Addition of calcium causes no vesicle aggregation, while zeta potential values indicate that Ca^{++} neutralizes the (slightly) negative SUV surface (Table 1).

AFM scans (Fig. 2d) together with the separation distance when two surfaces were in contact (Fig. 4c) indicate that vesicles of the 5-component mixture form flat bilayers with phase-separated domains (dimensions of order 10 – 100 nanometers) distributed irregularly on the bilayer. Egg SM and saturated long-chain PC lipids can form gel-state domains by tight alkyl chain packing and therefore are phase-separated from fluid phase composed of unsaturated PC lipids, similarly to "rafts" on biological membranes[47]. The hybrid POPC, with one saturated and one unsaturated tail, preferentially accumulates at the interface between the gel and liquid-crystalline phases, reducing the packing incompatibility and line tension between the two phases, further stabilizing small domains in the bilayer[48, 49]. After introducing 2 mM $Ca(NO_3)_2$, larger phase-separated domains appear on the bilayer – possibly because calcium binds laterally more strongly to Egg SM and DPPC than to POPC and DOPC[48], while the height of the patches is ca. 0.8 nm higher than the surroundings (Fig. 2f), attributed to the height difference between bilayers in gel and liquid-crystalline states[50].

Normal force profiles and friction vs. load behavior between layers for the L5 system are shown in Figs. 4c and 4d, respectively, where the friction is measured from traces such as in Fig. 3d.

Normal force profiles (Fig. 4c) show a similar trend to the L2 mixture (Fig. 4a). No significant repulsion is observed until two bilayers are in close contact at D ca. 13 nm; on increasing load before and after adding calcium, the bilayer thickness reaches a "hard-wall" at 10.4 ± 0.8 and 8.9 ± 0.8 nm, respectively, while following hemifusion, D decreases to 5.1 ± 1.1 and 4.6 ± 0.8 nm respectively. Even more marked than before, adding calcium to the system strongly increases the critical normal load triggering hemifusion from 15.6 ± 11.6 to 831.0 ± 122.3 mN/m in Fig. 4d, again equivalent to pressures of some MPa.

Prior to hemifusion, the friction is extremely low (at shear-trace noise levels) with $\mu \approx 10^{-4}$ both before and after adding 2 mM calcium (Fig. 4d). Immediately following hemifusion in the absence of calcium, μ increases ca. 50-fold (to $\mu \approx 5\times10^{-3}$). At the much higher loads and pressures leading to hemifusion in the presence of 2 mM calcium, we observed a "rigid-coupling" of two surfaces, indicating that the sliding friction exceeds the range applied shear force (F_s > 300 μN), corresponding to $\mu \geq$ ca. 3×10^{-2}.

L8 mixture: DPPC:POPC:DOPC:POPE:Egg SM:O-LPC:Chol:DPPA (1:1:1:1:1:1:1:0.1, molar ratio)

The third system consists of essentially all the major PL groups identified in synovial joints, at roughly their proportions as measured on articular cartilage surfaces[21], though it is not possible to include all the different lipids identified. Besides the 5-PL species in L2, a lyso-PC (O-LPC), cholesterol (chol), and a negatively charged PL (DPPA, 1.2 mol%) are also included in this system. Lyso-PC, with a conical configuration (positive curvature), is more likely to assemble in the outer leaflet of vesicles, and inhibits membrane fusion[51]. Chol is ubiquitous in PL membranes, acting as lateral spacers between the hydrophobic tails, and modulating their properties[52]. It is also found in synovial fluid[53], has an affinity to different PLs in the decreasing order SM > PC > PE, and it also preferentially interacts with saturated PCs over unsaturated ones, which facilitates their lateral segregation[54, 55, 56]. Adding chol to single-component PCs promotes bilayer hemifusion[16]. The gel-state negatively-charged PL, DPPA, not only brings negative charges to the gel-state patches but also shows particularly strong interaction with cations, particularly multi-valent cations, such as Ca^{++}[57]. We emphasize however, as considered further in the Discussion, that although all these lipid types are found in joints, it is not known whether they comprise part of the lubricating boundary layers on articulating cartilage *in vivo*.

DLS measurements (Table 1) show that the L8 vesicles are monodispersed and somewhat negatively charged. Adding calcium induces aggregation of liposomes, revealed by multiple peaks with larger sizes and a higher polydispersity (Fig. S3), as well as a slight reduction in the ζ-potential. On adsorption to mica (likely via dipole-charge interactions between the zwitterionic headgroups and the negatively-charged substrate), the liposomes rupture and form a planar layer with round phase-separated domains with diameter in the range of tens of nanometers (Fig. 2g). After adding 2 mM $Ca(NO_3)_2$, larger phase-separated gel-state patches are observed, and the height

of these domains are ca. 1-2 nm higher than the surroundings (Figs. 2h and 2i). This may arise from calcium binding strongly to adjacent anionic PLs, thus promoting a tighter packing of alkyl chain in the membrane and a thicker hydrophobic region ("condensing effect")[50, 58]. Force profiles for the L8 mixture are shown in Figs. 4e and 4f.

The normal force profiles in Fig. 4e show that monotonic repulsion (> 0.05 mN/m) between the L8 layers starts at larger surface separations (50 ± 10 nm) than was the case for L2 and L5, and may be attributed to loosely-trapped vesicles between the surface-attached bilayers. This is consistent with the profile shape which suggests rapid squeezing out of the loosely-attached liposomes at relatively low normal loads (ca. 10 mN/m). As F_n/R increases beyond ca. 10 mN/m the surfaces approach to separation D ~ 10 nm characteristic of a bilayer on each surface, and approach further slightly as normal load increases, until hemifusion occurs. As for L2 and L5, hemifusion of the compressed L8 bilayers is strongly suppressed and moved to higher pressures by the presence of calcium. Thus, hemifusion is observed at critical normal loads 48.5 ± 34.6 (in the range of 19.1 – 157.1) mN/m and 384.8 ± 111.5 (in the range of 241.3 – 610.1) mN/m before and after adding 2 mM calcium salt, while D decreases from 8.1 ± 0.8 and 7.0 ± 1.1 nm to 2.6 ± 0.5 and 3.1 ± 0.4 nm, respectively.

The measured friction (Fig. 4f) prior to hemifusion is also quite low, with friction coefficients $\mu \approx 10^{-4}$ up to mean contact pressure (0.6 – 3.0 MPa). Most of the critical loads (and thus contact pressures, see below) at hemifusion are somewhat lower than for the L2 and L5 mixtures, so that addition of cholesterol, lysoPC, and the anionic DPPA is seen to promote hemifusion relative to these other mixtures. In the presence of 2 mM calcium, friction increases strongly upon hemifusion

so that the two surfaces become rigidly coupled on lateral motion of the top one (corresponding in this case to $\mu \geq$ ca. 0.07), similar to the observation for the L5 layers.

Discussion and conclusions

The main findings of this work concern the synergy that may arise (see Introduction) using multicomponent lipid mixtures as lubricating boundary layers at the monovalent and divalent salt concentrations typical of physiological conditions in joints. In particular, use of the 5-component lipid mixture L5 leads to a lubricating layer which is significantly more robust to loading and shear than either the 2-component L2 or the 8-component L8 mixtures. This result, discussed below, is both unexpected and strongly suggestive, shedding light on the possible origin of the proliferation of lipid-types in joints from the view-point of cartilage lubrication. To appreciate this, it is instructive first to consider the effect of the presence of calcium on the interactions between the lipid- coated surfaces.

Effect of Calcium

Calcium ions are naturally present in joints at the 2 mM level[40], as in this study; the present measurements, both with and without added calcium salt, reveal directly its effect on lipid-based lubricating boundary layers, attributed to underlie the very low friction of articular cartilage[1, 2, 19]. The effect of the Ca^{++} ions on the interaction of the lipid mixture bilayers with the negatively-charged substrate (mica) is relevant, recalling that the *in-vivo* articular cartilage - while complex and very different to mica - is net negatively charged[59, 60] Likewise hyaluronan, attached at the cartilage surface, which has been proposed to complex with lipids to form its lubricating boundary

layer[1, 2], is also negatively charged. Thus, the lipid mixtures in our experiments are exposed to a similarly net-negatively-charged substrate as lipids in synovial joints, and one might expect that their interaction with it would be similarly affected by divalent cations.

Intuitively, one might have expected that the anionic divalent ions would bridge the opposing lipid layers through adhesive dipole-charge or charge-charge interactions. Indeed, the aggregation induced by Ca^{++} ions for vesicles of the L8 mixture (Table 1) indicates that such bridging occurs between the negatively-charged DPPA headgroups. Adhesive bridging might be expected to increase frictional dissipation as the surfaces slide, due to hysteretic bond breakage and reformation[12]. In contrast to this, our results reveal the opposite, counterintuitive effect of added physiological-level concentrations of calcium for all three mixtures studied, i.e., is that it actually improves the lubrication, by suppressing the hemifusion of opposing bilayers up to much higher loads than is the case in the absence of such ions. This renders the bilayers more robust to loading and shear and maintains the low-dissipation slip-plane between the hydrated PL headgroups to higher pressures. It thus suppresses the higher friction expected were slip to occur at (hydrophobic) tail-tail or bilayer-substrate interface following hemifusion.

To understand this suppression, consider that hemifusion is initiated when the stresses applied to interacting lipid bilayers deform them laterally, and, if there are defects or PL height mismatch in the bilayers, hydrophobic tails are exposed and van der Waals attraction between opposing hydrophobic tails could trigger hemifusion[61]. Thus we attribute the hemifusion suppression to the fact that the added calcium increases the *intra*-layer cohesion by bridging adjacent zwitterionic phosphocholine, leading also to a higher areal density of the lipids[57]. This increased cohesion

implies that larger loads/pressures are then needed to induce hemifusion. Our findings that Ca^{++} ions suppress hemifusion differ from a previous report that physiological level calcium promotes hemifusion of supported PL membranes[62]. The difference arises because in the previous study an asymmetric bilayer was used, where the lower leaflet rigidly anchored the outer, negatively-charged, mixed-lipid leaflet to the substrate, and the Ca^{++} ions bridged the two bilayers strongly to induce hemifusion. This contrasts with our study where calcium ions strengthened the much weaker bilayer/substrate interaction, while their intra-layer interactions within the essentially-neutral upper leaflets, enhanced by Ca^{++} as described above, rendered them more robust against hemifusion.

Lipid synergy in articular cartilage lubrication

The central question that this study addresses, as posed in the Introduction, is whether the presence of many different lipid types in synovial joints could, apart from any other biological roles that they play, lead to synergy in the boundary lubrication of articular cartilage. In other words, could the presence of a particular mix of lipids in the boundary-layer coating the cartilage, composed of those lipids present in the joint, result in optimal lubrication, in the sense of lower friction up to the highest (physiological) contact pressures? To answer this question comprehensively would require the examination of an impractically-large number of different combinations both of lipid classes (PC, PE, SM, cholesterol, etc.) and variations within each class (e.g. tail lengths, degree of unsaturation, etc.). Our purpose here however is not to identify such an optimal mix of lipids in the boundary layer, but to establish whether, based on our results above, together with earlier work, and the consideration of the role of calcium present in joints, such synergy is possible based on lipids that have been identified in synovial joints. This is indeed directly shown by our observations on lubrication by boundary layers of the L2, L5, and L8 lipid mixtures: in Fig. 5 we summarize the

critical loads at hemifusion with boundary layers of these three different mixtures. We plot the critical loads rather than the estimated pressures at hemi-fusion, since the former are accurately measured while the latter are estimated, with relatively large errors as described earlier. Moreover, since our experimental configurations – mica curvature and effective glue-layer modulus - are similar for all the SFB experiments, we expect the critical loads to correspond closely to the critical contact stresses at hemifusion, which normalizes the results of our measurements to macroscopic contacts.

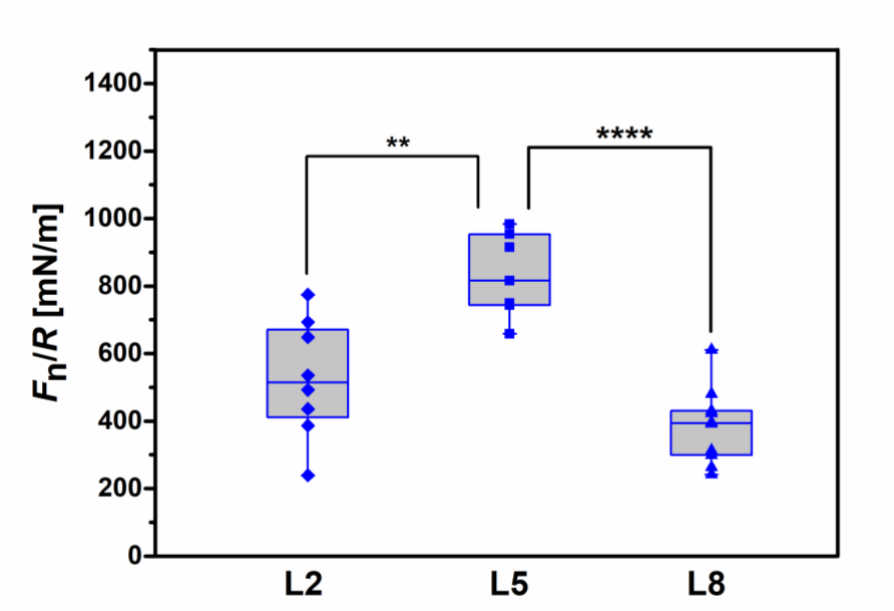

Figure 5. Normalized forces at the critical loads for hemifusion in the presence of physiological-level calcium for the three systems. Data are presented as box plots, whereas each box shows the interquartile range and the line inside represents the median. ** $p \leq 0.01$, **** $p \leq 0.0001$. Statistical analysis (unpaired *t* test) was performed using GraphPad Prism.

As seen clearly in Fig. 5, the boundary layers composed of the L5 mixture, comprising DPPC, POPC, DOPC, POPE, and Egg SM in equimolar concentrations, can provide low friction ($\mu \lesssim 10^{-4}$) prior to hemifusion at mean critical loads that are some 50% and 100% higher than with boundary

layers composed of the L2 or L8 mixtures respectively. Thus a clear synergy arising from the multiplicity of lipids is achieved in this case. This superior lubrication ability of L5 arises by adding to the L2 mixture (POPC and POPE) the additional lipids DPPC, DOPC, and Egg SM. The mere addition of more different lipid types is not in itself the origin of the better lubrication, as seen for L8 where the components of L5 are further augmented by other lipid types found in synovial joints, but where the lubrication is very significantly inferior to that of L5 as seen in Fig. 5. Our point is not that L5 represents the actual composition of lubricating boundary layers on articular cartilage, nor even that it is the best possible combination of the lipids used in the present study (Fig. S1 and Table S1) for forming lubricating boundary layers. Rather, the fact that a particular combination of lipids that are present in synovial joints, as in L5, provides superior lubrication – in the sense of a lubricating layer that is more robust to pressure and shear - than other combinations, is an unequivocal proof-of-concept that the proliferation of lipids in joints may indeed provide lubrication synergy.

We are now in a position to consider why the lubrication provided by the L5 boundary layers is superior to that of the L2 or L8 boundary layers. The three additional lipids in L5 relative to L2, DPPC, DOPC, and Egg SM, all have highly hydrated phosphocholine headgroups (more highly-hydrated than the phospho-ethanolamine headgroup of POPE[63]), contributing to their efficient friction-reducing ability[10, 11], while the high T_M of DPPC and Egg SM (Table S1) may contribute to the layer robustness. Such an explanation appears too simplistic, however, since it is not obvious that in a multi-lipid layer the lipid properties are simply additive. It is also clear, by examining the results for boundary layers composed of L8 (Figs. 4e and 4f), whose boundary lubrication is inferior to both L5 and L2, that merely increasing the number of lipids comprising a boundary layer does

not necessarily improve its lubricating properties. Rather, the presence of the negatively-charged DPPA in L8 may lead to the bilayer hemi-fusion at lower loads (relative to L2 and L5), due to bridging by Ca^{++} ions, and suggests that DPPA, despite its presence in synovial joints, may not be a significant component of the lubricating boundary layers on cartilage. At the same time, negative charges in the boundary layers may have the positive attribute of enabling Ca^{++} bridging to the negatively-charged cartilage surface[60] (which may also expose negatively-charged HA), thereby enhancing their adhesion to the substrate. Indeed, it is possible to imagine both "pros" and "cons" for each of the lipids used in this study, as briefly indicated in Table 2.

Table 2. Brief summary of some lubrication attributes of main lipid types used in this study, and their "pros" and "cons" with respect to boundary lubrication by lipid layers.

Lipid	" Pros"	"Cons"
Gel-state saturated PCs (e.g. DPPC)	Highly hydrated headgroups[13], robust bilayers, strong interaction with divalent cations and consequent stronger attachment to negatively charged substrates[64]	High friction following hemifusion[18], slow to heal following damage[65]
Liquid-state (unsaturated) PCs (e.g. POPC, DOPC)	Highly hydrated headgroups[42], heal rapidly following damage[10, 18], low friction on negatively-charged substrate following hemifusion[17]	Less robust bilayers; weaker attachment to negatively charged substrates[17]
Unsaturated PEs (e.g. POPE)	Stronger intra-layer headgroup interaction[44], resisting hemifusion[66]	Weaker headgroup hydration, non-lamellar-forming lipid[63], slow to heal following damage[66]
Sphingomyelins	Stronger intra-layer headgroup interaction resisting hemifusion[11], highly hydrated headgroups[67]	Likely to induce phase-separation with liquid-state PC lipids[31]
Negatively charged PLs (e.g. DPPA)	Charge promotes binding to negatively-charged substrate via Ca^{++} bridging[68]	Less highly hydrated[69]
Single tailed lipids (e.g. O-LPC)	Enhance the surface hydration of a PL bilayer[70]	Non-lamellar forming lipid by itself[71]

Cholesterol	Increases bilayer strength of fluid state lipids (such as unsaturated lipids)[56]	Poorly hydrated by itself, promotes hemifusion of PC bilayers[16]

A lipid-exposing lubricating boundary layer in synovial joints would then ideally possess the following attributes: the lipids would be strongly attached to the articular cartilage surface or complexed with HA molecules attached at that surface, to provide structural stability; they would form robust layers exposing highly-hydrated headgroups at the outer surface of the boundary layer, to provide low friction via the hydration lubrication mechanism; it would resist hemifusion when compressed at physiological pressures against a similar opposing layer; and it would possess rapid self-healing properties in case of any damage and wear (inevitable in any system where surfaces rub against each other). It can be seen from the above discussion and Table 2 that a suitable combination of lipids that are found in synovial joints (Fig. 3a and Table S1) can in principle address these requirements. Although, as noted, one cannot assume a simple additivity of properties in such a combination, our results – as summarized in Fig. 5 – show that L5 possesses these attributes significantly more than L2 and very significantly more than L8. But could this behaviour have been *a priori* predicted? We think this is doubtful: it is not possible to combine or add properties of single-lipid bilayers to predict the lubrication behaviour of a multi-lipid mixture in a persuasive manner.

In view of the complexity of property-additivity and the consequent difficulty of heuristically-identifying optimal combinations based just on their single-lipid properties as in Table 2, we propose a different approach to get insight into lipid mixtures that may have better boundary lubrication properties. This relies on molecular dynamics (MD) to probe both hemifusion and

frictional properties of bilayers consisting of different mixtures. Here we provide a proof of concept of such a scheme. Very recently we used MD to evaluate friction between two (single component) POPC lipid bilayers sliding past each other[72,73], both in the absence and presence of transverse electric fields across them, and this approach can readily be extended also to friction between bilayers consisting of lipid mixtures as in the present study. For probing the likelihood of *hemifusion* of bilayers, a different approach is used. A well-known indicator of impending hemifusion is the formation of a stalk structure between interacting membranes (i.e. lipid bilayers)[74-76], as schamtically shown in fig. 6C below. The development of such a stalk structure may be monitored graphically, and its likelihood may be gauged by evaluating the potential of mean force (PMF) at different values of the reaction coordinate ξ_{ch} corresponding to different stages of the stalk formation[74], with higher potentials corresponding to a lower likelihood of hemifusion. As proof of concept that this may yield insight into the lubrication properties of lipid mixture bilayers, we carried out such an MD simulation for the L2 and L5 lipid mixtures in this study, using the same MD protocols as in ref.[74], with hydration levels n_w = either 5 or 12 water molecules/lipid, which respectively represent the critical hydration level for hemifusion and the full hydration level. The results are presented in fig. 6. Fig. 6D shows that the PMF for the L5 mixture is significantly higher than for the L2 mixture, i.e. it predicts clearly that L5 better resists hemifusion than L2. This prediction arising from the MD calculations is exactly what the experimental SFB results show, as summarized in fig. 5: it could not have been predicted a priori based simply on qualitative properties of the single lipid bilayers as described in Table 2. This proof-of-concept demonstration thus strongly supports the notion that MD may be a powerful tool in gaining insight into nature's multi-lipid synergy in boundary lubrication of cartilage.

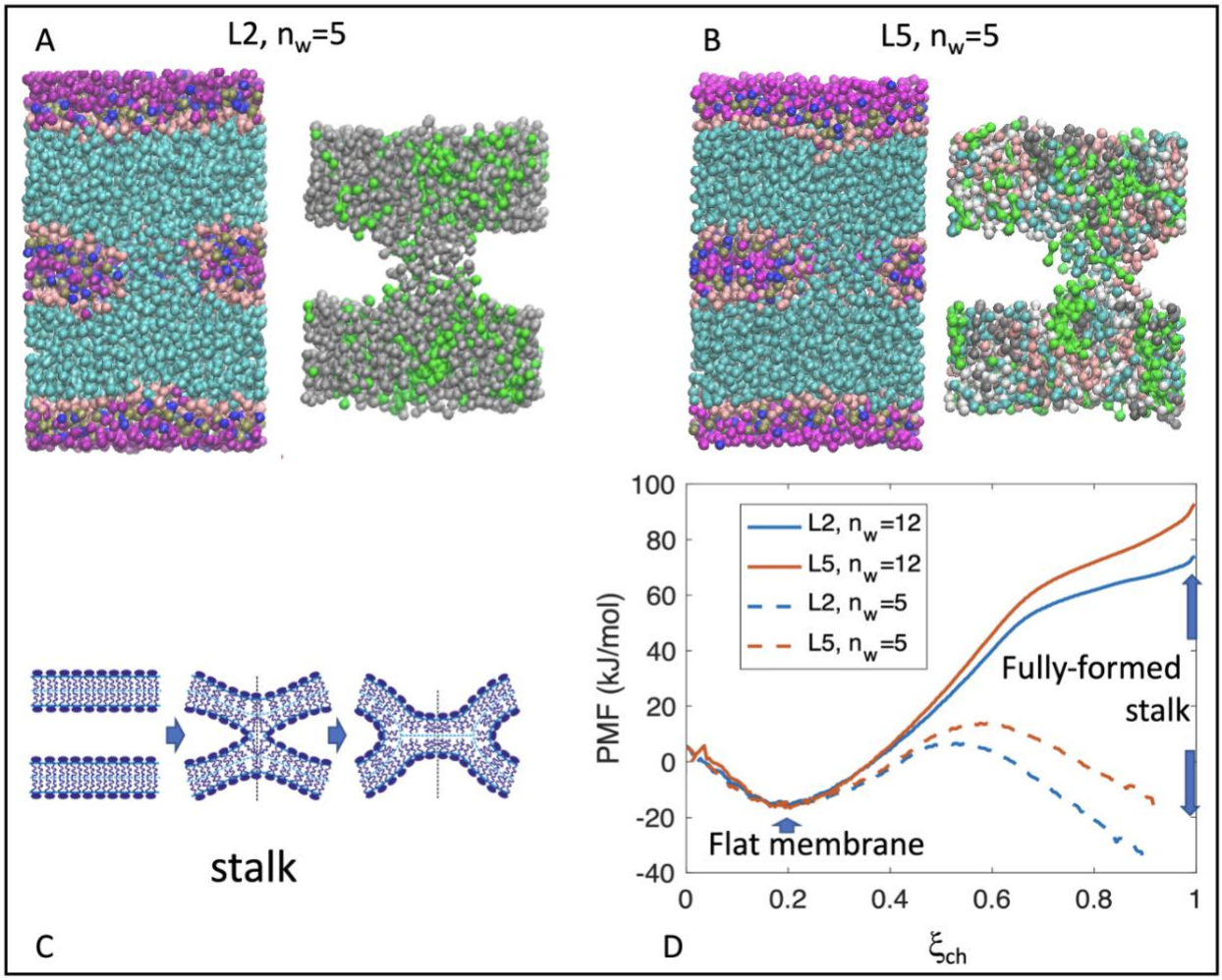

Figure 6. MD simulations of stalk formation in L2 and L5 mixtures. (A) and (B) illustrate graphically the stalk formation in the two mixtures at hydration levels n_w = 5 water molecules per lipid. (A) Left: magenta: water; cyan: acyl tails; gold: phosphate; blue: choline headgroup; pink: glycerol moieties. Right (acyl tails only): grey: POPC; green POPE. (B) Left: magenta: water; cyan: acyl tails; gold: phosphate; Blue: choline headgroup; pink: glycerol moieties. Right (acyl tails only): grey: SM (egg sphingomyeline); pink: POPC; green DPPC; white: DOPC; cyan: POPE. (C) Schematically showing how two interacting bilayers undergo hemifusion via intermediate stalk formation. (D) The potential of mean force (PMF) for L2 and L5 plotted as a function of the reaction coordinate ξ_{ch} (extent of stalk formation). Both n_w = 5 and n_w = 12 hydration levels are shown.

To conclude: we have shown that mixtures of lipids present in synovial joints may form boundary layers that possess excellent lubrication properties – comparable with those of healthy joints up to physiological pressures – while at the same time they may combine desirable features of their different components. By revealing that particular combinations of these lipids (e.g. L5) can be significantly superior as lubricating layers compared to other combinations with either more (L8) or fewer (L2) components, we unambiguously demonstrate the possibility of multi-lipid synergy. While we don't claim to have identified the optimal composition of such a layer, it is nonetheless clear from our results on a limited sample of synovial joint lipids that such an optimal composition is possible. This goes some way towards accounting for the proliferation of different lipid types in healthy synovial joints: purely from a lubrication point of view, essential for joint homeostasis, such a proliferation is clearly beneficial. Importantly, we were able to show, in a proof-of-concept demonstration, that molecular dynamics simulations are able to predict the relative robustness against hemifusion of different lipid mixtures (specifically, that L5 is less likely to hemifuse than L2, and that it is thus a better boundary lubricant at higher pressures, which was indeed one of our key observations). In the light of recent suggestions[2] that intra-articularly (IA) injected liposomes may serve to augment or repair the body's natural biolubrication mechanisms at the articular cartilage surface, our results may also point how to identify and implement optimal liposome compositions for such IA administration.

Conflict of interest

The authors declare no competing interest.

Acknowledgement

We thank the European Research Council (Advanced Grant CartiLube 743016), the McCutchen Foundation, the Israel Science Foundation – National Natural Science Foundation of China joint research program (Grant 3618/21), the Israel Ministry of Science and Technology (Grant 3-15716), and the Israel Science Foundation (Grant 1229/20) for financial support. This work was made possible partly through the historic generosity of the Perlman family.

References

1. Seror J, Zhu L, Goldberg R, Day AJ, Klein J. Supramolecular synergy in the boundary lubrication of synovial joints. *Nature Communications* **6**, 6497 (2015).

2. Jahn S, Seror J, Klein J. Lubrication of Articular Cartilage. *Annual Review of Biomedical Engineering* **18**, 235-258 (2016).

3. Hilšer P, Suchánková A, Mendová K, Filipič KE, Daniel M, Vrbka M. A new insight into more effective viscosupplementation based on the synergy of hyaluronic acid and phospholipids for cartilage friction reduction. *Biotribology* **25**, (2021).

4. Murakami T, Yarimitsu S, Nakashima K, Sawae Y, Sakai N. Influence of synovia constituents on tribological behaviors of articular cartilage. *Friction* **1**, 150-162 (2013).

5. Ateshian GA. The role of interstitial fluid pressurization in articular cartilage lubrication. *Journal of Biomechanics* **42**, 1163-1176 (2009).

6. Schmidt TA, Gastelum NS, Nguyen QT, Schumacher BL, Sah RL. Boundary lubrication of articular cartilage: Role of synovial fluid constituents. *Arthritis & Rheumatism* **56**, 882-891 (2007).

7. Goldberg R, Schroeder A, Silbert G, Turjeman K, Barenholz Y, Klein J. Boundary Lubricants with Exceptionally Low Friction Coefficients Based on 2D Close-Packed Phosphatidylcholine Liposomes. *Advanced Materials* **23**, 3517-3521 (2011).

8. Lin W, *et al.* Lipid-hyaluronan synergy strongly reduces intrasynovial tissue boundary friction. *Acta Biomaterialia* **83**, 314-321 (2019).

9. Duan Y, Liu Y, Li J, Feng S, Wen S. AFM Study on Superlubricity between Ti6Al4V/Polymer Surfaces Achieved with Liposomes. *Biomacromolecules* **20**, 1522-1529 (2019).

10. Sorkin R, Kampf N, Zhu L, Klein J. Hydration Lubrication and Shear-Induced Self-Healing of Lipid Bilayer Boundary Lubricants in Phosphatidylcholine Dispersions. *Soft Matter* **12**, 2773-2784 (2016).

11. Cao Y, Kampf N, Lin W, Klein J. Normal and shear forces between boundary sphingomyelin layers under aqueous conditions. *Soft Matter* **16**, 3973-3980 (2020).

12. Briscoe WH, Titmuss S, Tiberg F, Thomas RK, McGillivray DJ, Klein J. Boundary lubrication under water. *Nature* **444**, 191-194 (2006).

13. Sorkin R, Kampf N, Dror Y, Shimoni E, Klein J. Origins of extreme boundary lubrication by phosphatidylcholine liposomes. *Biomaterials* **34**, 5465-5475 (2013).

14. Yang L, Zhao X, Ma Z, Ma S, Zhou F. An Overview of Functional Biolubricants. *Friction*, (2022).

15. Lin W, Klein J. Recent Progress in Cartilage Lubrication. *Adv Mater* **33**, 2005513 (2021).

16. Sorkin R, Kampf N, Klein J. Effect of Cholesterol on the Stability and Lubrication Efficiency of Phosphatidylcholine Surface Layers. *Langmuir* **33**, 7459-7467 (2017).

17. Cao Y, Kampf N, Kosinska MK, Steinmeyer J, Klein J. Interactions Between Bilayers of Phospholipids Extracted from Human Osteoarthritic Synovial Fluid. *Biotribology* **25**, 100157 (2021).

18. Cao Y, Kampf N, Klein J. Boundary Lubrication, Hemifusion, and Self-Healing of Binary Saturated and Monounsaturated Phosphatidylcholine Mixtures. *Langmuir* **35**, 15459-15468 (2019).

19. Hills BA, Butler BD. Surfactants identified in synovial fluid and their ability to act as boundary lubricants. *Annual of Rheumatic Disease* **43**, 641-648 (1984).

20. Saikko V, Ahlroos T. Phospholipids as Boundary Lubricants in Wear Tests of Prosthetic Joint Materials. *Wear* **207**, 86-91 (1997).

21. Sarma AV, Powell GL, LaBerge M. Phospholipid composition of articular cartilage boundary lubricant. *J Orthop Res* **19**, 671-676 (2001).

22. Matei CI, *et al.* Ultrastructural Analysis of Healthy Synovial Fluids in Three Mammalian Species. *Microscopy and Microanalysis* **20**, 903-911 (2014).

23. Kosinska MK, *et al.* A Lipidomic Study of Phospholipid Classes and Species in Human Synovial Fluid. *Arthritis & Rheumatism* **65**, 2323-2333 (2013).

24. Proost P, *et al.* Sphingolipids in Human Synovial Fluid - A Lipidomic Study. *Plos One* **9**, e91769 (2014).

25. Hills BA. Oligolamellar Lubrication of Joints by Surface Active Phospholipid. *The Journal of Rheumatology* **16**, 82-91 (1989).

26. Hills BA. Boundary lubrication in vivo. *Proc Inst Mech Eng H* **214**, 83-94 (2000).

27. Wu C-L, Kimmerling KA, Little D, Guilak F. Serum and synovial fluid lipidomic profiles predict obesity-associated osteoarthritis, synovitis, and wound repair. *Scientific Reports* **7**, 44315 (2017).

28. Mustonen A-M, *et al.* Distinct fatty acid signatures in infrapatellar fat pad and synovial fluid of patients with osteoarthritis versus rheumatoid arthritis. *Arthritis Research & Therapy* **21**, (2019).

29. Zhu L, Seror J, Day AJ, Kampf N, Klein J. Ultra-low friction between boundary layers of hyaluronan-phosphatidylcholine complexes. *Acta Biomaterialia* **59**, 283-292 (2017).

30. Lin W, *et al.* Cartilage-inspired, lipid-based boundary-lubricated hydrogels. *Science* **370**, 335-338 (2020).

31. Heberle FA, Feigenson GW. Phase Separation in Lipid Membranes. *Cold Spring Harbor Perspectives in Biology* **3**, a004630-a004630 (2011).

32. Yang J, Calero C, Bonomi M, Martí J. Specific Ion Binding at Phospholipid Membrane Surfaces. *Journal of Chemical Theory and Computation* **11**, 4495-4499 (2015).

33. Melcrová A, *et al.* The complex nature of calcium cation interactions with phospholipid bilayers. *Scientific Reports* **6**, 38035 (2016).

34. Shi X, *et al.* Ca^{2+} regulates T-cell receptor activation by modulating the charge property of lipids. *Nature* **493**, 111-115 (2012).

35. Issa ZK, Manke CW, Jena BP, Potoff JJ. Ca^{2+} bridging of apposed phospholipid bilayers. *J Phys Chem B* **114**, 13249-13254 (2010).

36. McCutchen CW. Mechanism of Animal Joints Sponge-hydrostatic and Weeping Bearings. *Nature* **184**, 1284-1285 (1959).

37. Olson F, Hunt CA, Szoka FC, Vail WJ, Papahadjopoulos D. Preparation of liposomes of defined size distribution by extrusion through polycarbonate membranes. *Biochim Biophys Acta* **557**, 9-23 (1979).

38. Lin W, Klein J. Direct Measurement of Surface Forces: Recent Advances and Insights. *Applied Physics Reviews* **8**, 031316 (2021).

39. Kosinska MK. Boundary Lubricants in Osteoarthritic Synovial Fluid.). Justus-Liebig-University Giessen (2012).

40. Madea B, Kreuser C, Banaschak S. Postmortem biochemical examination of synovial fluid — a preliminary study. *Forensic Sci Int* **118**, 29-35 (2001).

41. Richter RP, Bérat R, Brisson AR. Formation of Solid-Supported Lipid Bilayers An Integrated View. *Langmuir* **22**, 3497–3505 (2006).

42. Kučerka N, Tristram-Nagle S, Nagle JF. Structure of Fully Hydrated Fluid Phase Lipid Bilayers with Monounsaturated Chains. *Journal of Membrane Biology* **208**, 193-202 (2006).

43. Gurtovenko AA, Vattulainen I. Lipid Transmembrane Asymmetry and Intrinsic Membrane Potential Two Sides of the Same Coin. *J Am Chem Soc* **129**, 5358-5359 (2007).

44. Leekumjorn S, Sum AK. Molecular Simulation Study of Structural and Dynamic Properties of Mixed DPPC/DPPE Bilayers. *Biophysical Journal* **90**, 3951-3965 (2006).

45. Roy MT, Gallardo M, Estelrich J. Influence of Size on Electrokinetic Behavior of Phosphatidylserine and Phosphatidylethanolamine Lipid Vesicles. *Journal of Colloid and Interface Science* **206**, 512-517 (1998).

46. Her C, *et al.* The Charge Properties of Phospholipid Nanodiscs. *Biophysical Journal* **111**, 989-998 (2016).

47. Lingwook D, Simons K. Lipid Rafts As a Membrane-Organizing Principle. *Science* **327**, 46-50 (2010).

48. Szekely O, Schilt Y, Steiner A, Raviv U. Regulating the Size and Stabilization of Lipid Raft-like Domains and Using Calcium Ions as Their Probe. *Langmuir* **27**, 14767-14775 (2011).

49. Palmieri B, Safran SA. Hybrid Lipids Increase the Probability of Fluctuating Nanodomains in Mixed Membranes. *Langmuir* **29**, 5246-5261 (2013).

50. Alessandrini A, Facci P. Phase transitions in supported lipid bilayers studied by AFM. *Soft Matter* **10**, 7145-7164 (2014).

51. Yeagle PL, Smith FT, Young JE, Flanagan TD. Inhibition of Membrane Fusion by Lysophosphatidylcholine. *Biochem* **33**, 1820-1827 (1994).

52. Ohvo-Rekilä H, Ramstedt B, Leppimäki P, Slotte JP. Cholesterol interactions with phospholipids in membranes. *Prog Lipid Res* **41**, 66-97 (2002).

53. Bole GG. Synovial fluid lipids in normal individuals and patients with rheumatoid arthritis. *Arthritis & Rheumatism* **5**, 589-601 (1962).

54. Niu S-L, Litman BJ. Determination of Membrane Cholesterol Partition Coefficient Using a Lipid Vesicle–Cyclodextrin Binary System. *BIophysical Journal* **83**, 3408-3415 (2002).

55. Van Dijck PWM. Negatively charged phospholipids and their position in the cholesterol affinity sequence. *Biochimica et Biophysica Acta* **555**, 89-101 (1979).

56. Engberg O, *et al.* The Affinity of Cholesterol for Different Phospholipids Affects Lateral Segregation in Bilayers. *Biophysical Journal* **111**, 546-556 (2016).

57. Pedersen UR, Leidy C, Westh P, Peters GH. The effect of calcium on the properties of charged phospholipid bilayers. *Biochimica et Biophysica Acta (BBA) - Biomembranes* **1758**, 573-582 (2006).

58. Yaghmur A, Sartori B, Rappolt M. The role of calcium in membrane condensation and spontaneous curvature variations in model lipidic systems. *Phys Chem Chem Phys* **13**, 3115-3125 (2011).

59. Laver-Rudich Z, Silvermann M. Cartilage surface charge A possible determinant in aging and osteoarthritic processes. *Arthritis & Rheumatism* **28**, 660-670 (1985).

60. Minassian A, O'Hare D, Parker KH, Urban JP, Warensjo K, Winlove CP. Measurement of the charge properties of articular cartilage by an electrokinetic method. *J Orthop Res* **16**, 720-725 (1998).

61. Helm CA, Israelachvili JN, McGuiggans PM. Role of Hydrophobic Forces in Bilayer Adhesion and Fusion. *Biochem* **31**, 1794-1805 (1992).

62. Banquy X, Kristiansen K, Lee DW, Israelachvili JN. Adhesion and hemifusion of cytoplasmic myelin lipid membranes are highly dependent on the lipid composition. *Biochimica et Biophysica Acta (BBA) - Biomembranes* **1818**, 402-410 (2012).

63. Rappol M, Hicke A, Bringezu F, Lohner K. Mechanism of the Lamellar/Inverse Hexagonal Phase Transition Examined by High Resolution X-Ray Diffraction. *Biophys J* **84**, 3111-3122 (2003).

64. Szekely O, *et al.* The Structure of Ions and Zwitterionic Lipids Regulates the Charge of Dipolar Membranes. *Langmuir* **27**, 7419-7438 (2011).

65. Wang M, *et al.* The effect of temperature on supported dipalmitoylphosphatidylcholine (DPPC) bilayers: Structure and lubrication performance. *Journal of Colloid and Interface Science* **445**, 84-92 (2015).

66. Benz M, Gutsmann T, Chen N, Tadmor R, Israelachvili J. Correlation of AFM and SFA Measurements Concerning the Stability of Supported Lipid Bilayers. *Biophys J* **86**, 870-879 (2004).

67. Watanabe N, Suga K, Slotte JP, Nyholm TKM, Umakoshi H. Lipid-Surrounding Water Molecules Probed by Time-Resolved Emission Spectra of Laurdan. *Langmuir* **35**, 6762-6770 (2019).

68. Richter RP, Brisson AR. Following the formation of supported lipid bilayers on mica: a study combining AFM, QCM-D, and ellipsometry. *Biophys J* **88**, 3422-3433 (2005).

69. Bach D, Miller IR. Hydration of phospholipid bilayers in the presence and absence of cholesterol. *Biochim Biophys Acta* **1368**, 216-224 (1998).

70. Alves M, Bales BL, Peric M. Effect of lysophosphatidylcholine on the surface hydration of phospholipid vesicles. *Biochim Biophys Acta* **1778**, 414-422 (2008).

71. Inoue S, Uchihashi T, Yamamoto D, Ando T. Direct observation of surfactant aggregate behavior on a mica surface using high-speed atomic force microscopy. *Chem Commun* **47**, 4974-4976 (2011).

72. Jin, D., Zhang, Y. & Klein, J. Electric-field-induced topological changes in multilamellar and in confined lipid membranes. Preprint at *arXiv:2303.08551* (2023).

73. Jin, D. & Klein, J. Tuning friction via topologically electro-convoluted lipid-membrane boundary layers. Preprint at *arXiv:2303.08555* (2023).

74. Poojari, C. S., Scherer, K. C. & Hub, J. S. Free energies of membrane stalk formation from a lipidomics perspective. *Nature Communications* **12**, 6594 (2021). https://doi.org:10.1038/s41467-021-26924-2

75. Yang, L. & Huang, H. W. Observation of a Membrane Fusion Intermediate Structure. *Science* **297**, 1877-1879 (2002). https://doi.org:10.1126/science.1074354

76. Smirnova, Y. G., Marrink, S.-J., Lipowsky, R. & Knecht, V. Solvent-exposed tails as prestalk transition states for membrane fusion at low hydration. *Journal of the American Chemical Society* **132**, 6710-6718 (2010). https://doi.org:10.1021/ja910050x